


RESEARCH

Open Access



AIMP2 accumulation in brain leads to cognitive deficits and blood secretion in Parkinson's disease

Heejeong Kim^{1,2†}, Jeong-Yong Shin^{1,2†}, Sangwoo Ham^{1,2,3}, Ji Hun Kim^{1,2}, Gum Hwa Lee⁴, Nae-Eung Lee⁵, Hee-Tae Kim⁶, Seok Hyun Cho⁷, Sangseong Kim⁸ and Yunjong Lee^{1,2*} 

Abstract

Background Propagation of neuronal α -synuclein aggregate pathology to the cortex and hippocampus correlates with cognitive impairment in Parkinson's disease (PD) dementia and dementia with Lewy body disease. Previously, we showed accumulation of the parkin substrate aminoacyl-tRNA synthetase interacting multifunctional protein-2 (AIMP2) in the temporal lobe of postmortem brains of patients with advanced PD. However, the potential pathological role of AIMP2 accumulation in the cognitive dysfunction of patients with PD remains unknown.

Methods We performed immunofluorescence imaging to examine cellular distribution and accumulation of AIMP2 in brains of conditional AIMP2 transgenic mice and postmortem PD patients. The pathological role of AIMP2 was investigated in the AIMP2 transgenic mice by assessing Nissl-stained neuron counting in the hippocampal area and Barnes maze to determine cognitive functions. Potential secretion and cellular uptake of AIMP2 was monitored by dot blot analysis and immunofluorescence. The utility of AIMP2 as a new PD biomarker was evaluated by dot blot and ELISA measurement of plasma AIMP2 collected from PD patients and healthy control followed by ROC curve analysis.

Results We demonstrated that AIMP2 is toxic to the dentate gyrus neurons of the hippocampus and that conditional AIMP2 transgenic mice develop progressive cognitive impairment. Moreover, we found that neuronal AIMP2 expression levels correlated with the brain endothelial expression of AIMP2 in both AIMP2 transgenic mice and in the postmortem brains of patients with PD. AIMP2, when accumulated, was released from the neuronal cell line SH-SY5Y cells. Secreted AIMP2 was taken up by human umbilical vein endothelial cells. Consistent with the fact that AIMP2 can be released into the extracellular space, we showed that AIMP2 transgenic mice have higher levels of plasma AIMP2. Finally, ELISA-based assessment of AIMP2 in plasma samples from patients with PD and controls, and subsequent ROC curve analysis proved that high plasma AIMP2 expression could serve as a reliable molecular biomarker for PD diagnosis.

[†]Heejeong Kim and Jeong-Yong Shin contributed equally to this work.

*Correspondence:
Yunjong Lee
ylee69@skku.edu

Full list of author information is available at the end of the article



Conclusions The pathological role in the hippocampus and the cell-to-cell transmissibility of AIMP2 provide new therapeutic avenues for PD treatment, and plasma AIMP2 combined with α -synuclein may improve the accuracy of PD diagnosis in the early stages.

Keywords AIMP2, Conditional transgenic mice, Lewy body dementia, Intercellular protein transmission, Blood biomarker, Diagnosis

Background

Parkinson's disease (PD) is the most common neurodegenerative movement disorder, affecting 1% of those aged >60 years [1]. Age-dependent and progressive degeneration of midbrain dopamine-producing neurons is responsible for the cardinal clinical motor symptoms in patients with PD [2]. As the disease progresses, patients also experience a number of non-motor symptoms involving several brain subregions other than the ventral midbrain [3]. Both PD dementia (PDD) and dementia with Lewy bodies (DLB) involve α -synuclein pathologies in wide brain regions although the time course of motor and cognitive symptoms differ [4]. α -Synuclein aggregation and its propagation through neural connection have been implicated as cellular and molecular mechanisms of Braak staging of disease progression [5]. To understand PD pathologies more thoroughly, it is critical to study signaling pathways related to α -synuclein aggregation. Notably, we have shown that α -synuclein aggregation pathology can be potentiated by reciprocal interaction with the parkin substrate aminoacyl-tRNA synthetase interacting multifunctional protein-2 (AIMP2) [6]. AIMP2 accumulation has clinical relevance since the brains (cortex, striatum, and ventral midbrain) of patients with PD have higher AIMP2 expression than controls [6–8]. Transgenic mice expressing AIMP2 in brain neurons develop age-dependent and selective dopamine neurodegeneration with characteristic motor dysfunction [8]. The transgenic mice express exceptionally high levels of AIMP2, especially in the cortex and hippocampus subregions, and α -synuclein aggregation pathology is observed in whole brain lysates of eight-month-old AIMP2 transgenic mice [6, 8]. Although AIMP2 has been reported to be elevated and aggregated in the postmortem temporal lobe of the brains of patients with PD, its potential pathological role in cognitive dysfunction in PDD or DLB has not been investigated.

The diagnosis of PD relies heavily on the semi-quantitative scoring of PD-associated motor and non-motor symptoms (unified PD-rating scale, UPDRS) by trained physicians. DatScan brain imaging of dopaminergic axon terminal loss in the striatum can aid in PD diagnosis [9]. However, this brain imaging requires systemic injection of a radiolabeled ligand and is not easily accessible to patients because only a large hospital can maintain this high-cost imaging instrument. It has been shown that the misdiagnosis of PD is up

to 35% when confirmed by Lewy body immunohistochemical analysis of postmortem brains [10]. Moreover, UPDRS scoring or brain imaging can diagnose PD only when there is degeneration of 4–60% of dopaminergic neurons [11]. Consequently, there has been tremendous unmet medical need for molecular diagnostic biomarkers that can reflect the pathologic events relevant to PD, such as α -synuclein aggregation. α -Synuclein was shown to be detectable in several biofluid samples, including cerebrospinal fluid (CSF), blood, and saliva, indicating its release into extracellular spaces [12]. CSF α -synuclein levels have been reproducibly demonstrated to be decreased in patients with PD by several groups [12]. Although studies on blood α -synuclein as a PD biomarker remain controversial [12], additional blood biomarkers in combination with α -synuclein could improve the diagnostic accuracy. Several disease-associated proteins, which can be misfolded and aggregated, have been shown to have cell-to-cell transmission (e.g., α -synuclein and tau) [13]. Along with α -synuclein, the parkin substrate AIMP2 has the ability to self-oligomerize and form amyloid aggregates when its levels increase in mouse brains [6]. Similar to α -synuclein, AIMP2 is a potential blood biomarker that is pathologically and clinically relevant in PD. However, it is largely unknown whether AIMP2 can be secreted and transferred between cells, and thus whether it can be detected in the blood as a biomarker for diagnosing brain pathologies involving AIMP2 accumulation that may occur in PD.

In this study, we observed high AIMP2 expression in both neurons and brain endothelial cells in the postmortem temporal lobes of patients with PD. Neuronal AIMP2 overexpression resulted in high endothelial AIMP2 accumulation in transgenic mice, with elevated blood AIMP2 levels in an age-dependent manner. We also showed that AIMP2 can be secreted from a neuronal cell line at high levels and that this secreted AIMP2 can be taken up by an endothelial cell line. ELISA measurements of AIMP2 in human plasma samples revealed the potential of AIMP2 as a reliable blood biomarker for diagnosing PD. Finally, transgenic mice overexpressing neuronal AIMP2 displayed hippocampal neurodegeneration and cognitive impairment, supporting the pathological role of AIMP2 in PDD and DLB.

Materials and methods

Human postmortem brain and plasma samples

Post-mortem brain sections (temporal lobes from patients with PD and age-matched healthy controls) were obtained from the Brain Body Donation Program. Detailed information on the demographic characteristics of the brain samples has been described previously [6]. The biospecimens and data used in the dot blot analysis of blood AIMP2 were provided by the Biobank of Jeonbuk National University Hospital, Inje University Paik Hospital, Gyeongsang National University Hospital, Chungbuk National University Hospital, Keimyung University Hospital, and members of the Korea Biobank Network, which is supported by the Ministry of Health, Welfare, and Family Affairs. All samples derived from the Korea Biobank Network were obtained with informed consent using institutional review board-approved protocols. The plasma samples used in the ELISA analysis of blood AIMP2 were obtained from Hanyang University Hospital. The use of human plasma samples for detection of the blood biomarker AIMP2 was approved by the appropriate institutional review board (SKKU 2018-07-018-001; HY-2021-06-040)).

Antibodies

The following primary antibodies were used: rabbit antibody against AIMP2 (Proteintech; #10424-1-AP, 1:5,000), mouse antibody against MAP2 (Sigma-Aldrich; #M4403, 1:5,000), rabbit antibody against MAP2 (Abcam; #ab32454, 1:5,000), mouse antibody against CD31 (BD Biosciences; #550274, 1:1,000), and rabbit antibody against GFP (Cell Signaling Technology; #2555S, 1:5,000). The following secondary antibodies were used: horseradish peroxidase (HRP)-conjugated goat antibody to rabbit IgG (Genetex, #GTX-213110-01, 1:5,000), Alexa Fluor 488 donkey anti-mouse IgG (Invitrogen; #A21202, 1:1,000), Alexa Fluor 568 donkey anti-mouse IgG (Invitrogen #A10037, 1:1,000), Alexa Fluor 488 goat anti-rabbit IgG (Invitrogen; #A11008, 1:1,000), Alexa Fluor 568 donkey anti-rabbit IgG (Invitrogen; #A10042, 1:1,000), biotin-conjugated goat antibody to rabbit IgG (Vector Laboratories; #BA-1000, 1:1,000), and HRP-conjugated mouse antibody to β -actin (Sigma-Aldrich; #A3854, 1:10,000).

ELISA analysis of blood AIMP2

The capture antibody was diluted in the coating buffer and applied to the plates followed by blocking buffer. Standards and samples were prepared in blocking buffer, added to wells and incubated at room temperature for 1 h. The plate was then washed and the detection antibody diluted in blocking buffer was added to each well, followed by a 2 h incubation. Then, the streptavidin-HRP working solution was applied for a 30-minute incubation.

After washing, 5,5'-Tetramethylbenzidine substrate solution was added for a 30-minute incubation, followed by stop solution. Absorbance was measured at 450 nm. The resultant data were analyzed utilizing either a log-log or 4-parameter curve fitting method.

ROC curve analysis

GraphPad Prism software (GraphPad, ver. 8.4) was used for further analysis of optical density values from dot blot and ELISA assays. In this process, the OD values or actual concentration values for the control group were entered in column A, whereas the OD values for the PD group were entered in column B. Following data entry, the analysis option was selected within the data table window; specifically, the ROC curve analysis was chosen. Within the ROC dialogue box, columns containing the results for both the control and PD groups were specified. In addition, the desired output format, either a Fraction or Percentage, is designated. This configuration was used for the analysis. As a result of this analysis, pertinent outcomes were obtained, including the AUC value, as well as metrics pertaining to Sensitivity and Specificity. The ROC curve itself was also generated.

Statistical analysis

Quantitative data are presented as the mean \pm standard error of the mean (SEM). The normality of the data was tested using the Shapiro–Wilk test. Statistical significance was assessed either via nonparametric two-tailed Mann–Whitney test for two-group comparisons, or analysis of variance (ANOVA) with Tukey's *post hoc* analysis for the comparison of more than three groups. Results were considered statistically significant at $p < 0.05$. Pearson's correlation coefficient analysis was used for the correlation studies. Statistical analyses were performed using the Prism software (GraphPad, ver. 8.4).

Detailed other methods can be found in the supplementary information.

Results

Neuronal AIMP2 accumulation correlates with brain endothelial AIMP2 accumulation in postmortem brains of patients with Parkinson's disease

Marked elevation of aminoacyl-tRNA synthetase interacting multifunctional protein-2 (AIMP2) in MAP2-positive cortical neurons was found in the postmortem temporal lobes of patients with PD compared with age-matched control subjects (Fig. 1A, B). While we were investigating the expression of AIMP2 in postmortem brain sections, we found distinct patterns of AIMP2 expression that differed from the expression signals from MAP2-positive neurons. It turned out that PD brains expressed higher levels of AIMP2 in CD31-positive brain endothelial cells than age-matched control

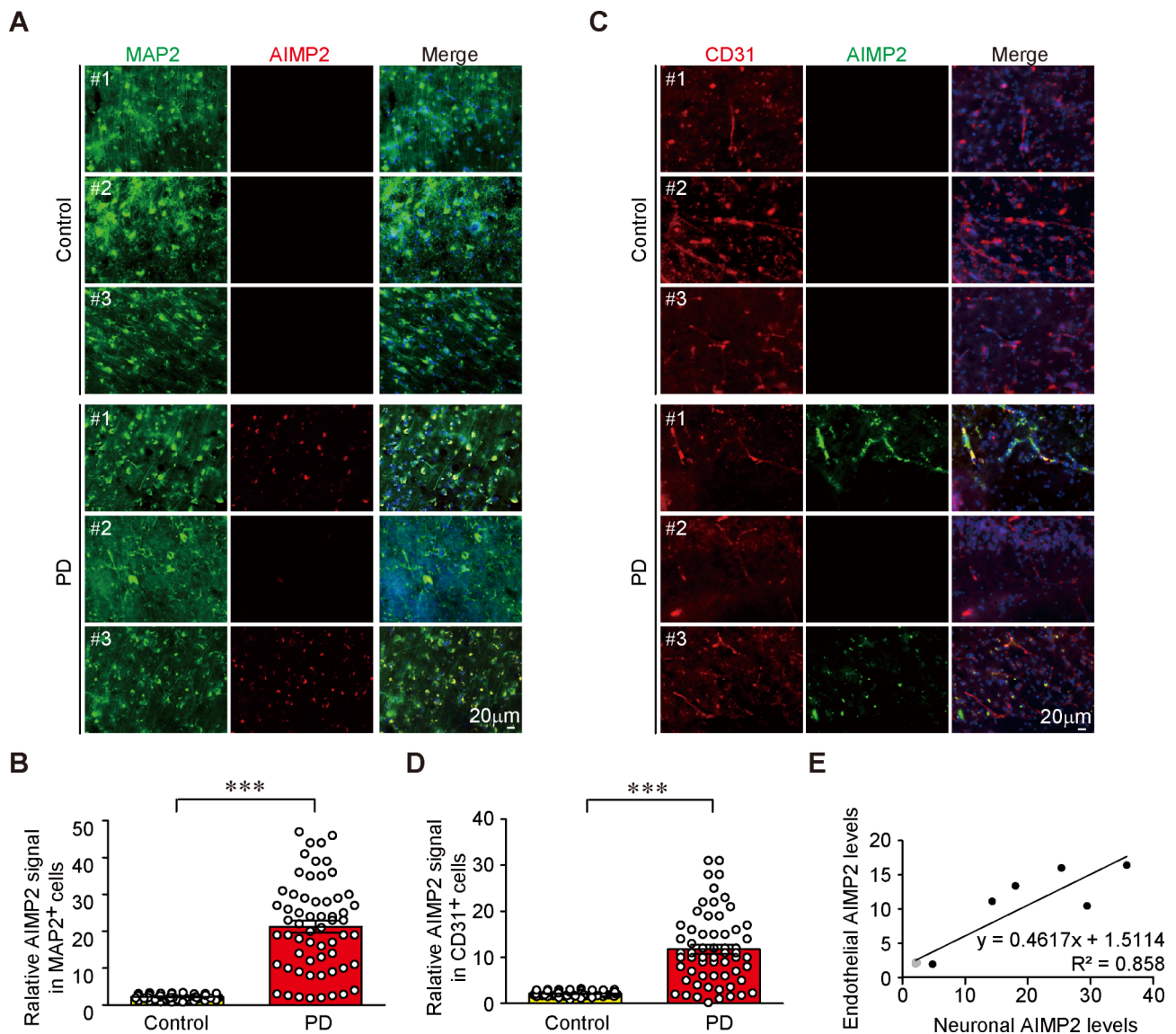


Fig. 1 AIMP2 accumulation in neurons and endothelium of Parkinson's disease brains. **(A)** Expression of AIMP2 in postmortem temporal lobe sections from patients with Parkinson's disease (PD) and age-matched controls monitored by immunofluorescence. Neurons were costained with neuron marker microtubule-associated protein 2 (MAP2) and AIMP2 antibodies. Scale bar = 20 μ m. **(B)** Quantification of AIMP2 immunofluorescence signals in MAP2-positive neurons from brain sections of patients with PD and age-matched control ($n = 60$ cells from six controls and 60 cells from six PD). **(C)** Expression of AIMP2 in postmortem temporal lobe sections from patients with PD and age-matched controls monitored by immunofluorescence. Endothelial cells were costained with CD31 and AIMP2 antibodies. Scale bar = 20 μ m. **(D)** Quantification of AIMP2 immunofluorescence signals in CD31-positive cerebral endothelial cells in brain sections of patients with PD and age-matched controls ($n = 60$ cells from six controls and 60 cells from six PD). **(E)** Pearson correlation analysis between neuronal and endothelial AIMP2 expression levels in control and PD brain sections. Control samples ($n = 6$): gray dots; PD samples ($n = 6$): black dots. Quantitative data are expressed as the mean \pm standard error of the mean (SEM), and statistical significance was determined using nonparametric two-tailed Mann–Whitney test. *** $p < 0.001$

as determined by co-immunofluorescence analysis (Fig. 1C and D). Moreover, there was a positive correlation between neuronal AIMP2 and brain endothelial AIMP2 expression (Fig. 1E). PD brains with high neuronal AIMP2 accumulation tended to exhibit endothelial AIMP2 accumulation (Fig. 1E).

Conditional transgenic mice expressing neuronal AIMP2 exhibited hippocampal neurodegeneration and cognitive impairment

Based on the neuronal accumulation of AIMP2 in the temporal lobes of patients with PD, the potential pathological role of AIMP2 in the hippocampus was examined. Conditional Tet-Off-transgenic mice expressing AIMP2 in the pan-neuronal population especially of

forebrains [8] were used to characterize the pathological consequences of AIMP2 accumulation in the cortex and hippocampus. Consistent with the previous characterization of this AIMP2 transgenic mouse line and other conditional transgenic mice using CamKII α -tTA as a driver [8, 14, 15], higher levels of AIMP2 accumulation were observed in the cortex and hippocampal brain subregions (CAs and dentate gyrus) of transgenic mice than in controls (Fig. 2A). Moreover, AIMP2 transgenic mice demonstrated robust AIMP2 expression mainly in MAP2-positive neuronal populations in the forebrain (Supplementary Fig. 1A, B). The extent of AIMP2 expression levels in MAP2-positive neurons was maintained at both two and six months of age (Supplementary Fig. 1A, C). Hippocampal AIMP2 accumulation selectively led to the age-dependent progressive degeneration of hippocampal neurons in the dentate gyrus. While there was no loss of CA1 neurons in both two- and six-month-old AIMP2 transgenic mice, the loss of dentate gyrus neurons in transgenic mice at six months of age was approximately 71% (Fig. 2B-D). Consistent with our previous report [8], there were no changes in the number of neurons in the cortical regions of AIMP2 transgenic mice at both two and six months of age (Supplementary Fig. 1D, E).

Wild-type and AIMP2 transgenic mice displayed similar open-field exploration activity (Supplementary Fig. 1F, G). The transgenic mice, however, developed an anxiety phenotype at six months of age, with an increased tendency to stay in the border areas compared to the center area of the open field arena (Supplementary Fig. 1H). And consistent with our previous study [8], AIMP2 Tg mice displayed marked impairment of motor coordination as evidenced by reduced retention time in the accelerating rotarod test (Supplementary Fig. 1I). Spatial learning and memory performance were assessed using the Barnes maze behavioral test. While control and two-month-old AIMP2 transgenic mice had no issues in learning or finding the target hole with the underneath hiding cage on the Barnes maze circle arena with 20 holes in the boundary, six-month-old AIMP2 transgenic mice showed spatial learning and memory deficits with no ability to find the target hole during the second and third Barnes maze test sessions with increased latency and travel distance (Fig. 2E, F, G). Taken together, these results indicate that neuronal AIMP2 accumulation in mice leads to selective and progressive dentate gyrus neurodegeneration in the hippocampus, with associated behavioral deficits in cognitive function. This *in vivo* finding suggests a potential pathological role of AIMP2 in cognitive impairment in PD and DLB with AIMP2 accumulation in the brain.

AIMP2 accumulation in a neuronal cell line results in its extracellular secretion and uptake by an endothelial cell line

AIMP2 accumulation was observed in brain endothelial cells and neurons in the postmortem PD temporal lobes (Fig. 1). Since AIMP2 aberrant accumulation has been implicated in neuronal degeneration and Lewy body formation [6, 8], we hypothesized that neuronal AIMP2 is secreted and subsequently transmitted to brain endothelial cells. To test this possibility, AIMP2 transgenic mice that expressed exogenous AIMP2 in a neuronal population driven by the CamKII α promoter were examined. To examine the endothelial AIMP2 expression, the fluorescence focus was adjusted to the endothelial marker CD31. High AIMP2 expression levels were found in CD31-positive endothelial cells of AIMP2 transgenic mice (Fig. 3A, B). This transfer of AIMP2 from neurons to endothelial cells appears to be age-dependent and progressive since the buildup of endothelial AIMP2 in AIMP2 transgenic mice was not obvious in two-month-old AIMP2 transgenic mice, and only manifested at six months of age (Fig. 3A, B).

To gain mechanistic insights into AIMP2 transfer from neurons to the endothelium, the potential release of AIMP2 from the neuroblastoma cell line, SH-SY5Y cells was examined. SH-SY5Y cells were transiently transfected with green fluorescent protein (GFP)-tagged AIMP2 (GFP-AIMP2), and its secretion was monitored in the culture media by dot blot analysis using an AIMP2 antibody. While no detectable AIMP2 protein secretion was observed from GFP-transfected SH-SY5Y cells, AIMP2 secretion was readily observed in the culture media of GFP-AIMP2 transfected SH-SY5Y cells (Fig. 3C). The AIMP2 concentration in the medium from SH-SY5Y cells transfected with GFP-AIMP2 was approximately 207 pg/mL (Fig. 3C, D), as calculated from the recombinant GST-AIMP2 standard calibration curve (Supplementary Fig. 2A, B). Dot blot assay using anti-GFP antibody confirmed secretion of GFP-tagged AIMP2 from GFP-AIMP2-transfected SH-SY5Y cells and further revealed no secretion of GFP alone from GFP-transfected SH-SY5Y cells (Fig. 3E, F). Whether AIMP2 secretion is associated with AIMP2 cellular accumulation was also examined. GFP-AIMP2 expression in SH-SY5Y cells was gradually increased by elevated doses of GFP-AIMP2 constructs when normalized to the endogenous AIMP2 (Supplementary Fig. 2C, D). When AIMP2 secretion into the culture medium of these experimental groups was monitored, AIMP2 secretion was found to be influenced by the extent of cellular AIMP2 accumulation (Fig. 3G, H).

Next, whether the secreted AIMP2 could penetrate endothelial cells was investigated. To determine this possibility, human umbilical vein endothelial cells

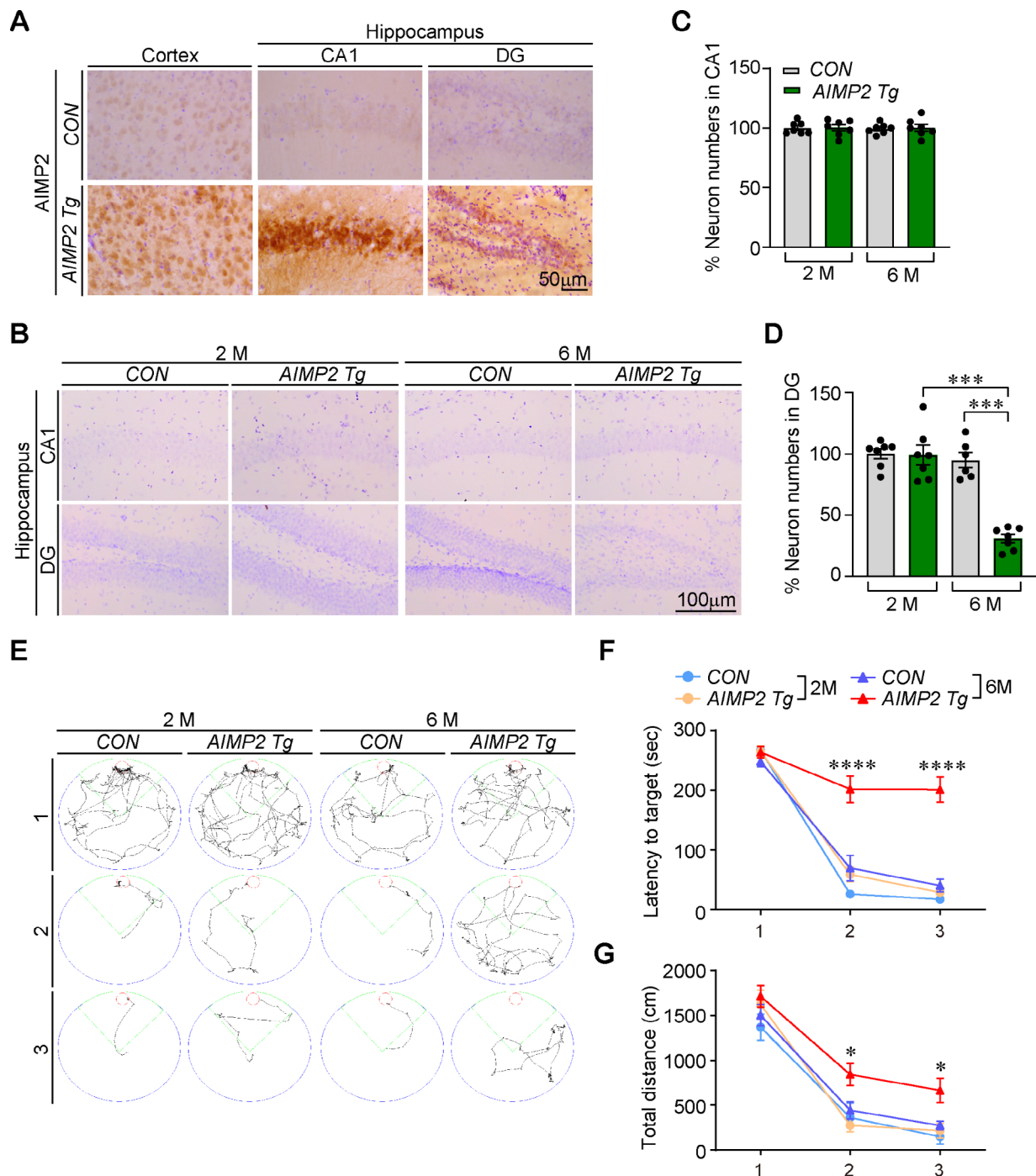


Fig. 2 Transgenic mice expressing AIMP2 in brain develop age-dependent cognitive dysfunction. **(A)** Representative immunohistochemistry images showing robust expression of AIMP2 in the cortex and hippocampus (CA1, and dentate gyrus (DG)) of AIMP2 transgenic mice (two months old) as compared to the age-matched control littermate. Scale bar = 50 μ m. **(B)** Nissl-stained hippocampal coronal sections from two- and six-month-old AIMP2 transgenic mice and age-matched control littermates. Representative images show CA1 and DG. Scale bar = 100 μ m. **(C)** Quantification of relative number of Nissl-positive neurons in the CA1 regions of hippocampus from two- and six-month-old AIMP2 transgenic mice and littermate controls ($n=7$ each group). **(D)** Quantification of relative number of Nissl-positive neurons in the DG regions of hippocampus from two- and six-month-old AIMP2 transgenic mice and littermate controls ($n=7$ each group). **(E)** Representative trace of mice finding the hiding cage (indicated as red circle) located underneath of the circular arena of the Barnes maze in repetitive trials (1 = the first training, 2 = on 3 days since the first training, 3 = 5 days since the second training) for AIMP2 transgenic mice and littermate controls of two and six months of age. **(F, G)** Assessment of spatial learning and memory, using the Barnes maze, as determined by the time and travel distance taken to find the hiding cage in the repeated trials (n = two-month-old Con: 5 male, 4 female; two-month-old Tg: 6 male, 3 female; six-month-old Con: 6 male, 6 female; six-month-old Tg: 5 male, 7 female). Quantitative data are expressed as the mean \pm SEM, and statistical significance was determined using ANOVA with Tukey's *post hoc* test. * $p < 0.05$, *** $p < 0.001$, and **** $p < 0.0001$

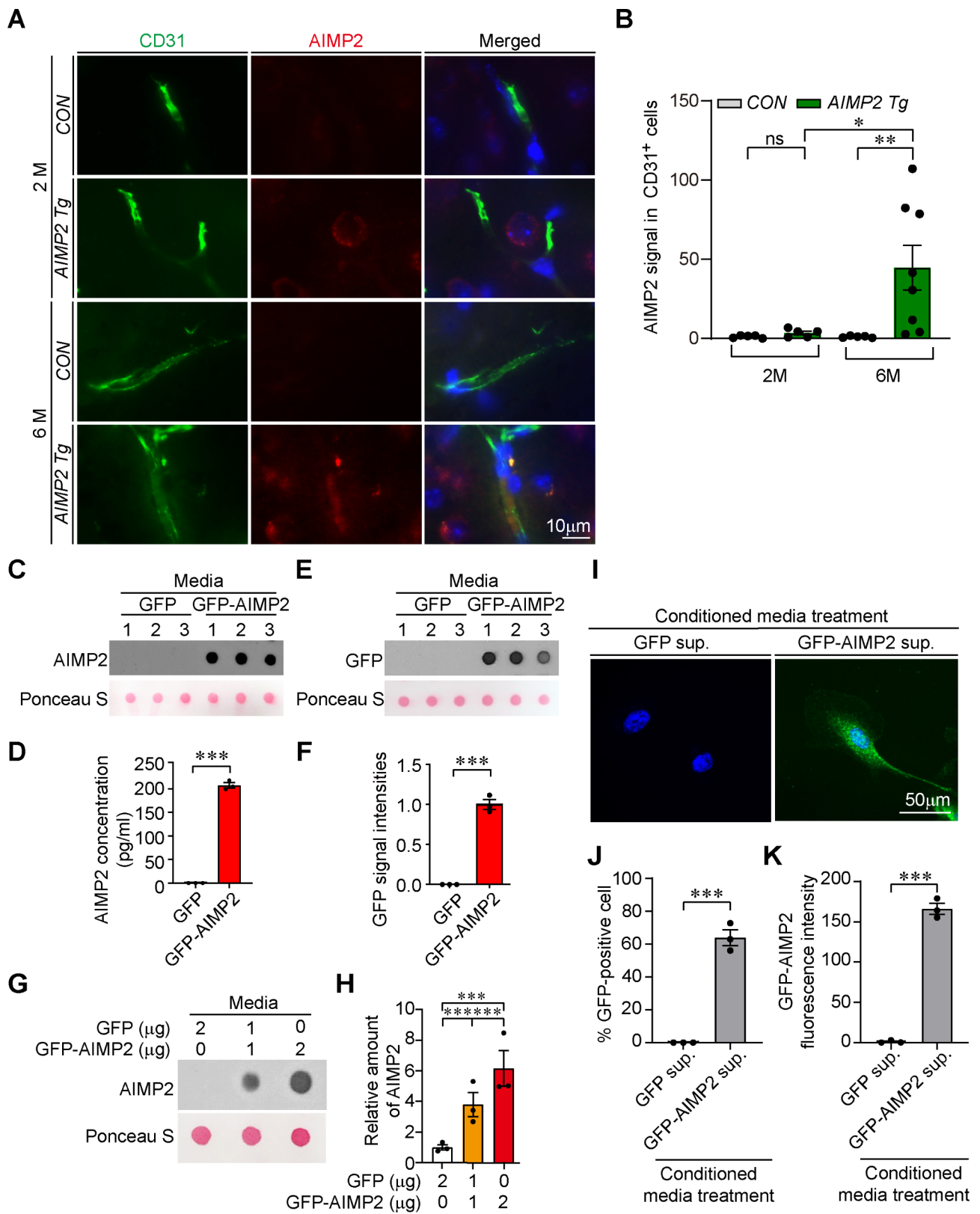


Fig. 3 (See legend on next page.)

(See figure on previous page.)

Fig. 3 Intracellular AIMP2 accumulation leads to AIMP2 secretion and intercellular transmission. **(A)** Representative immunofluorescence images of endothelial marker CD31 and AIMP2 in the cortical brain subregions from two- and six-month-old AIMP2 transgenic mice and age-matched littermate controls. The nucleus was counterstained with 4',6-diamidino-2-phenylindole dihydrochloride (DAPI). Scale bar = 10 μ m. **(B)** Quantification of AIMP2 signal intensities in CD31-positive brain endothelium in the indicated mouse groups ($n=5$ in two-month-age group, $n=5$ in control six-month-age group, and $n=8$ in AIMP2 Tg six-month-age group). **(C)** Anti-AIMP2 dot blot assessment of GFP-AIMP2 protein in the culture media from SH-SY5Y cells transiently transfected with either GFP or GFP-AIMP2 constructs. Ponceau staining was used to visualize the proteins in the culture media. Complete media was changed to serum-deprived media 24 h before analysis of AIMP2 secretion. **(D)** Quantification of secreted AIMP2 in the media from SH-SY5Y cells transfected with GFP or GFP-AIMP2 based on the dot blot result in the panel C ($n=3$ separate experiments per group). **(E)** Anti-GFP dot blot assessment of GFP-AIMP2 protein in the culture media from SH-SY5Y cells transiently transfected with either GFP or GFP-AIMP2 constructs. Ponceau staining was used to visualize the proteins in the culture media. Complete media was changed to serum-deprived media 24 h before analysis of AIMP2 secretion. **(F)** Quantification of relative anti-GFP dot blot optical densities for experimental groups in the panel E ($n=3$ separate experiments per group). **(G)** Dot blot assessment of AIMP2 protein in the culture media from SH-SY5Y cells transiently transfected with GFP-AIMP2 construct (0, 1, 2 μ g). Ponceau staining was used to visualize the proteins in the culture media. Complete media was changed to serum-deprived media 24 h before analysis of AIMP2 secretion. **(H)** Quantification of secreted AIMP2 in the media from SH-SY5Y cells transfected with the indicated combination of GFP and GFP-AIMP2 ($n=3$ separate experiments per group). **(I)** Representative immunofluorescence images showing GFP-AIMP2 uptake into HUVECs. HUVECs were treated with conditioned media (48 h) from GFP or GFP-AIMP2 transfected SH-SY5Y cells. Scale bar = 50 μ m. **(J)** Percentage GFP-positive HUVECs in the indicated experimental groups ($n=3$ separate experiments per group). **(K)** Quantification of GFP-AIMP2 immunofluorescence signals in HUVECs in the indicated experimental groups ($n=3$ separate experiments per group). Quantitative data are expressed as the mean \pm SEM, and statistical significance was determined by ANOVA with Tukey's *post hoc* test. * $p < 0.05$, ** $p < 0.01$ and *** $p < 0.001$. ns, non-significant

(HUVECs), were treated with conditioned media from either GFP transfected or GFP-AIMP2 transfected SH-SY5Y cells. The GFP signal was only detected in the cytoplasm of HUVECs treated with conditioned media from SH-SY5Y cells transiently transfected with GFP-AIMP2 (Fig. 3I-K). In contrast, there was no GFP signal in HUVECs that were treated with conditioned media from SH-SY5Y cells transfected with the control vector GFP (Fig. 3I-K). We obtained the same result of AIMP2 secretion from SH-SY5Y cells and uptake by HUVECs for FLAG-tagged AIMP2 (Supplementary Fig. 2E-K). This result suggests that AIMP2 can be released from cells when AIMP2 is accumulated, and this secreted AIMP2 can be taken up by an endothelial cell line.

Blood AIMP2 is increased in patients with PD and serves as a potential diagnostic biomarker

We showed AIMP2 accumulation in both neurons and brain endothelial cells of the postmortem PD patients' brains. Moreover, transgenic mice overexpressing robust AIMP2 mainly in the forebrain neurons exhibited a high AIMP2 signal in the brain endothelial cells at 6 months of age. Because these findings of this study suggest the ability of AIMP2 to be secreted and transmitted across cells, we reasoned that AIMP2 could be released into the blood stream when AIMP2 is accumulated in the brain neurons. To test this hypothesis, we sought to determine the AIMP2 concentrations in plasma samples from AIMP2 transgenic mice and age-matched littermate controls. First, an enzyme-linked immunosorbent assay (ELISA) was established for measuring plasma AIMP2 concentration and generating a calibration curve (Supplementary Fig. 3A, B). ELISA revealed an approximately 2.5-fold increase in plasma AIMP2 concentration in six-month-old AIMP2 transgenic mice compared to age-matched controls (Fig. 4A). While plasma AIMP2 concentration was approximately 2 pg/ μ L in wild-type control mice, it

increased up to 5 pg/ μ L in six-month-old AIMP2 transgenic mice (Fig. 4A). Two-month-old AIMP2 transgenic mice showed plasma AIMP2 levels comparable with age-matched controls (Fig. 4A), indicating that AIMP2 secretion and elevation in the blood are age-dependent and progressive.

Dot blot analyses were performed to determine AIMP2 concentrations in plasma samples collected from 24 patients with PD and 24 age-matched controls with musculo-skeletal diseases (Supplementary Fig. 3D and Fig. 4B). When normalized to Ponceau-stained total plasma proteins, a marked elevation of AIMP2 was observed in most of the plasma samples from patients with PD, while detectable AIMP2 was observed in plasma samples from only three controls (Fig. 4B, C). Quantification of normalized AIMP2 levels in the plasma revealed a significant elevation of AIMP2 in patients with PD (Fig. 4C). The potential of AIMP2 as a biomarker for PD diagnosis was evaluated using the receiver operating characteristic (ROC) curve analysis. The ROC curve analysis of the dot blot results showed that plasma AIMP2 can serve as an excellent diagnostic biomarker with high sensitivity and specificity (70.8% and 87.5% at 1.75 cutoff value, respectively) (Fig. 4D). To further validate plasma AIMP2 as a PD diagnostic biomarker, plasma samples from 42 patients with PD and age-matched healthy control subject (Supplementary Fig. 3E) were collected and analyzed using ELISA to determine the AIMP2 concentration (Fig. 4E). Consistent with the preliminary small group dot blot analysis, more than 1.62-fold elevation in plasma AIMP2 concentration was observed in patients with PD when compared to healthy controls (Fig. 4E). The AIMP2 plasma concentration was approximately 6.38 pg/ μ L in controls and this was elevated to an average of 10.44 pg/ μ L in patients with PD patients (Fig. 4E). AIMP2 plasma concentration in humans was slightly higher than that in mice. The AIMP2 as a diagnostic biomarker of PD was further evaluated using ELISA data from PD and control plasma

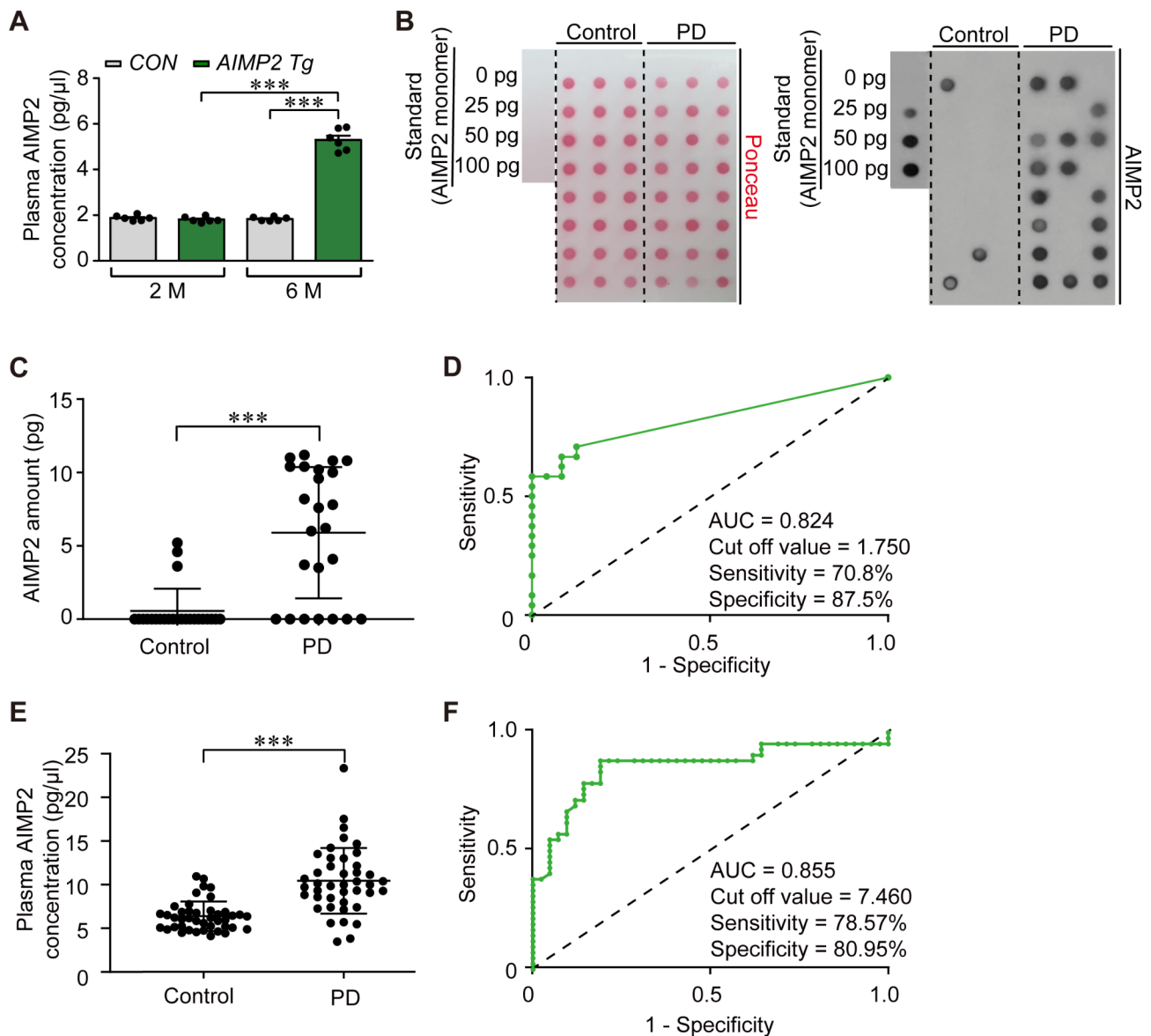


Fig. 4 Blood AIMP2 as a potential biomarker for Parkinson's disease diagnosis. **(A)** ELISA analysis of plasma AIMP2 levels in two- and six-month-old AIMP2 transgenic mice and age-matched littermate controls ($n=6$ per group). **(B)** Dot blot analysis of AIMP2 in plasma samples collected from patients with PD and age matched subjects with musculo-skeletal diseases (Control). Recombinant AIMP2 was used for standard generation and quantification. **(C)** Quantification of plasma AIMP2 levels in PD ($n=24$) and age-matched musculo-skeletal disease controls ($n=24$) determined by dot blot analysis. **(D)** Receiver operating characteristic (ROC) curve analysis of the data set in the panel C obtained from dot blot analysis. AUC, cut off value, specificity, and sensitivity were calculated and presented in the graph. **(E)** ELISA quantification of plasma AIMP2 in the additional plasma samples collected from patients with PD ($n=42$) and age matched healthy control subjects ($n=42$). **(F)** ROC curve analysis of the data set in the panel E obtained from ELISA analysis. AUC, cut-off value, specificity, and sensitivity are presented in the graph. Quantitative data are expressed as the mean \pm SEM, and statistical significance was determined by ANOVA with Tukey's *post hoc* test. *** $p < 0.001$

samples. Consistent with the previous preliminary analysis (Fig. 4D), ROC curve analysis revealed that plasma AIMP2 levels served as a reliable biomarker for PD diagnosis, with an area under the curve (AUC) of 0.855 (Fig. 4F). The sensitivity and specificity of PD diagnosis were 78.57%, and 80.95 at 7.46 a cutoff AIMP2 plasma value, respectively (Fig. 4F). These results together strongly suggest that PD can be reliably diagnosed using plasma AIMP2 concentration, which

can be efficiently measured by antibody-based dot blot or ELISA analysis.

Discussion

Pathological role of AIMP2 in hippocampal degeneration and cognitive deficits

In this study, the pathological causal role of aminoacyl-tRNA synthetase interacting multifunctional protein-2

(AIMP2) in hippocampal dentate gyrus neurodegeneration and cognitive impairment in mice was demonstrated. AIMP2 is a pathological substrate of the recessive PD gene parkin [16, 17]. AIMP2 accumulation in postmortem brains has been reported not only in autosomal recessive juvenile PD with parkin loss, but also in sporadic PD with inactivation of parkin E3 ligase activity [7, 17, 18]. Recent studies have shown that AIMP2 is coaggregated with α -synuclein in Lewy bodies in the brains of patients with advanced PD [6]. Moreover, the accumulation and aggregation of AIMP2 was also present in the temporal lobe subregions of postmortem brains of patients with advanced PD [6]. However, to date, the potential pathological role of AIMP2 in the hippocampus and cognitive dysfunction in PDD has not been investigated. Previously, conditional AIMP2 transgenic mice were characterized mainly by PD-related motor impairments [8]. However, potential cognitive deficits were not further explored, partly due to the lack of cortical neuron loss, although the potential functional decline of cortical neurons with AIMP2 accumulation cannot be excluded. The current study revealed that AIMP2 accumulation in the mouse brain induces spatial learning and memory deficits. Given that AIMP2 accumulation has been reported in the cortex of the postmortem brains of patients with advanced PD, AIMP2 may contribute to the dementia phenotypes of patients with PDD or DLB. The differential vulnerability of cortical and hippocampal neurons to AIMP2 accumulation was also identified. Consistent with our previous report [8], it was confirmed that cortical neurons were resistant to AIMP2-induced neurodegeneration at eight months of age. Even in the hippocampus, dentate gyrus neurons showed extensive degeneration in eight-month-old AIMP2 transgenic mice, while neurons in the CA1 (Fig. 3B, C) and CA2 (data not shown) regions were relatively spared. Although functional decline of spared cortical or CA neurons is possible in AIMP2 transgenic mice, cognitive decline in eight-month-old AIMP2 transgenic mice is likely due to the substantial loss of dentate gyrus neurons, because this hippocampal region is thought to be involved in episodic and spatial memory [19]. Since α -synuclein pathology was reported to be concentrated in CA2 regions of the hippocampus of patients with PDD and DLB [20], further histopathological characterization of AIMP2 aggregation or accumulation is necessary to explore the clinical relevance of AIMP2 in diverse neurodegenerative diseases with cognitive decline.

We showed that 6-month-old AIMP2 Tg mice displayed anxiety-like behavior in the open field test. It is, however, necessary to further evaluate this anxiety phenotype in AIMP2 Tg mice with more mice in each group to convincingly demonstrate this behavioral abnormality. In addition, considering the influence of gender

difference on anxiety [21], it would be informative to include behavior tests performed with the same gender in each experimental group.

AIMP2 accumulation overactivates PARP1 and kills dopaminergic neurons via parthanatos [20]. Moreover, AIMP2 misfolding and aggregation can induce α -synuclein coaggregation and neuronal loss [6]. Since this is the first report demonstrating that AIMP2 accumulation is responsible for dentate gyrus neuron loss and cognitive decline, it would be instructive to evaluate pharmacological inhibitors that block PARP1 activation or the AIMP2 aggregation process to determine if AIMP2-mediated hippocampal neurodegeneration can be prevented. This AIMP2-targeted therapeutic strategy might supplement current therapeutic trials targeting α -synuclein for PDD and DLB, and thus enhance therapeutic efficacy especially for those patients with AIMP2 accumulation in the brain.

Cell to cell transmission of AIMP2

Several disease-associated protein aggregates, such as α -synuclein and tau, have been shown to spread to the entire brain regions through cell-to-cell transmission [13]. Similarly, the current study revealed that the PD disease protein AIMP2 was secreted from SH-SY5Y cells when overexpressed. Secreted AIMP2 can penetrate endothelial cell lines. The findings suggest an underlying mechanism for the high AIMP2 expression observed in the neurons and endothelial cells of postmortem brains from patients with PD, and in the brains of transgenic mice expressing AIMP2 in neurons. It is, however, important to note that AIMP2 signal in CD31 cells could be originated from endogenous expression of endothelial AIMP2 under pathological conditions of PD. Moreover, additional validation using primary neuron culture system would be required to confirm neuronal secretion of AIMP2. To exclude potential interference of other proteins in conditioned media, it would be informative to use in vitro-prepared AIMP2 monomer or aggregate to evaluate potential transfer of different AIMP2 species to diverse cell types. Preformed α -synuclein fibrils can penetrate brain endothelial cells and influence their functions [22]. Examining the potential pathological effects of AIMP2 uptake on brain endothelial cell function would be informative. In addition, pathological extracellular α -synuclein has been shown to interact with neurons or surrounding microglia through specific interaction with a cognate receptor for α -synuclein aggregates [23, 24]. Pharmacological, immunological, or genetic intervention in receptor and α -synuclein interaction has been shown to be effective in the prevention of neuroinflammation and Lewy-like pathology propagation [24]. Since AIMP2 can be secreted into the extracellular space of the brain, it would be interesting to investigate the potential adverse

effects of AIMP2 on adjacent neurons and microglia. Given the presence of extracellular AIMP2 and its potential pathological role, specific antibodies against AIMP2 could be beneficial for blocking the interaction of AIMP2 with unidentified receptors on various cell types.

AIMP2 as a reliable biomarker for PD diagnosis

It is a novel finding that AIMP2 can be detected and that its levels are elevated in blood samples from patients with PD. PD brains showed correlation between AIMP2 expression in neurons and endothelial cells. Neuronal AIMP2 overexpression in mice also leads to AIMP2 accumulation in brain endothelial cells. Since only aged AIMP2 transgenic mice presented with elevated AIMP2 secretion in the plasma, it is highly likely that blood AIMP2 partly reflects the pathological and potentially neuronal accumulation of AIMP2 in the brain of patients with PD. The validity of AIMP2 as a reliable diagnostic tool for PD was confirmed using antibody-based dot blotting and ELISA. Plasma AIMP2 measurements in two separate and independent cohorts of patients with PD and controls from different institutions provided consistent and comparable specificity and sensitivity for PD diagnosis.

There is a tremendous need for reliable molecular biomarkers for PD diagnosis. Ideally, biomarkers should be assessed in relatively easily accessible biofluids such as blood. In addition, pathologically relevant biomarkers have advantages because disease onset can be detected years before substantial irreversible neurodegeneration occurs. Therefore, α -synuclein has been extensively studied as a potential biofluid-derived biomarker for PD diagnosis. While α -synuclein present in erythrocytes can hamper accurate measurement of plasma α -synuclein, a recent study of plasma exosomal α -synuclein, potentially derived from brain CSF, showed 70% diagnostic sensitivity and 52% specificity for PD [25]. Since plasma AIMP2 alone showed approximately 80% diagnostic sensitivity and specificity, application of a multi-marker panel, combining AIMP2, α -synuclein, and other plasma marker candidates, might further enhance the diagnostic accuracy. The establishment of a combined marker panel would also determine a precision therapeutic strategy, since both AIMP2 and α -synuclein are pathologically relevant disease proteins in the brain.

Supplementary Information

The online version contains supplementary material available at <https://doi.org/10.1186/s12967-024-05666-x>.

Supplementary Material 1

Author contributions

Y.L. conceived the hypotheses and supervised the study. H.K. and J-Y.S. performed most of the experiments and analyzed the data. S.H. and J.H.K.

performed the experiments and analyzed the data. G.H.L, N-E.L., H-T.K., S.H.C. and S.K. provided technical and material support. H.K., J-Y.S. Y.L. wrote the manuscript. All authors contributed to the final review of the manuscript and figures.

Funding

This research was supported by a grant from the Korea Dementia Research Project through the Korea Dementia Research Center (KDRC), funded by the Ministry of Health and Welfare and Ministry of Science and ICT, Republic of Korea (grant number: HU22C014300022). This research was also supported by National Research Foundation of Korea (NRF) grants funded by the Korean Ministry of Science and ICT (No. 2021M3H4A4079521). This research was also supported by a grant from the Korea Health Technology R&D Project through the Korea Health Industry Development Institute (KHIDI), funded by the Ministry of Health and Welfare, Republic of Korea (grant number: HI17C1711).

Data availability

The data that support the findings of this study are available on request from the corresponding author.

Declarations

Ethics approval and consent to participate

All animal experiments were approved by the Ethics Committee of Sungkyunkwan University and were conducted in accordance with all applicable international guidelines (SKKUIACUC2020-05-04-1). The use of human plasma samples was approved by the appropriate institutional review board (SKKU 2018-07-018-001; HY-2021-06-040).

Consent for publication

Not applicable.

Competing interests

S.H., and Y.L. are inventors of the patent related to this work (South Korea domestic patent no. 10-2252879, "Method for diagnosing Parkinson's disease using AIMP2 in blood plasma, composition therefor and kit containing the same"). The authors declare no conflicts of interest.

Author details

¹Department of Pharmacology, Sungkyunkwan University School of Medicine, Suwon 16419, Republic of Korea

²Samsung Medical Center (SMC), Sungkyunkwan University School of Medicine, Samsung Biomedical Research Institute, Suwon 16419, Republic of Korea

³ToolGen Inc, Seoul 08501, Republic of Korea

⁴College of Pharmacy, Chosun University, Gwangju 61452, Republic of Korea

⁵Department of Advanced Materials Science and Engineering, Sungkyunkwan University, Suwon, Gyeonggi-do 16419, Korea

⁶Department of Neurology, Hanyang University College of Medicine, Seoul 04763, Korea

⁷Department of Otorhinolaryngology-Head and Neck Surgery, Hanyang University College of Medicine, Seoul 04763, Korea

⁸Department of Biomedical Science and Engineering, Gwangju Institute of Science and Technology, Gwangju 61005, Republic of Korea

Received: 20 December 2023 / Accepted: 4 September 2024

Published online: 10 October 2024

References

1. Tysnes OB, Storstein A. Epidemiology of Parkinson's disease. *J Neural Transm* (Vienna). 2017;124:901–5.
2. Lang AE, Lozano AM. Parkinson's disease. First of two parts. *N Engl J Med*. 1998;339:1044–53.
3. Poewe W. Non-motor symptoms in Parkinson's disease. *Eur J Neurol*. 2008;15(Suppl 1):14–20.
4. Jellinger KA. Dementia with Lewy bodies and Parkinson's disease-dementia: current concepts and controversies. *J Neural Transm* (Vienna). 2018;125:615–50.

5. Burke RE, Dauer WT, Vonsattel JP. A critical evaluation of the Braak staging scheme for Parkinson's disease. *Ann Neurol*. 2008;64:485–91.
6. Ham S, Yun SP, Kim H, Kim D, Seo BA, Kim H, Shin JY, Dar MA, Lee GH, Lee YI et al. Amyloid-like oligomerization of AIMP2 contributes to alpha-synuclein interaction and lewy-like inclusion. *Sci Transl Med*. 2020;12.
7. Ko HS, Lee Y, Shin JH, Karuppagounder SS, Gadad BS, Koleske AJ, Pletnikova O, Troncoso JC, Dawson VL, Dawson TM. Phosphorylation by the c-Abl protein tyrosine kinase inhibits parkin's ubiquitination and protective function. *Proc Natl Acad Sci U S A*. 2010;107:16691–6.
8. Lee Y, Karuppagounder SS, Shin JH, Lee YI, Ko HS, Swing D, Jiang H, Kang SU, Lee BD, Kang HC, et al. Parthanatos mediates AIMP2-activated age-dependent dopaminergic neuronal loss. *Nat Neurosci*. 2013;16:1392–400.
9. Postuma RB, Berg D. Advances in markers of prodromal Parkinson disease. *Nat Rev Neurol*. 2016;12:622–34.
10. Rajput AH, Rozdilsky B, Rajput A. Accuracy of clinical diagnosis in parkinsonism—a prospective study. *Can J Neurol Sci*. 1991;18:275–8.
11. Fearnley JM, Lees AJ. Ageing and Parkinson's disease: substantia nigra regional selectivity. *Brain*. 1991;114(Pt 5):2283–301.
12. Atik A, Stewart T, Zhang J. Alpha-Synuclein as a biomarker for Parkinson's disease. *Brain Pathol*. 2016;26:410–8.
13. Uemura N, Uemura MT, Luk KC, Lee VM, Trojanowski JQ. Cell-to-cell transmission of tau and alpha-synuclein. *Trends Mol Med*. 2020;26:936–52.
14. Lin X, Parisiadou L, Gu XL, Wang L, Shim H, Sun L, Xie C, Long CX, Yang WJ, Ding J, et al. Leucine-rich repeat kinase 2 regulates the progression of neuro-pathology induced by Parkinson's-disease-related mutant alpha-synuclein. *Neuron*. 2009;64:807–27.
15. Yetman MJ, Jankowsky JL. Wild-type neural progenitors divide and differentiate normally in an amyloid-rich environment. *J Neurosci*. 2013;33:17335–41.
16. Corti O, Hampe C, Koutnikova H, Darios F, Jacquier S, Prigent A, Robinson JC, Pradier L, Ruberg M, Mirande M, et al. The p38 subunit of the aminoacyl-tRNA synthetase complex is a parkin substrate: linking protein biosynthesis and neurodegeneration. *Hum Mol Genet*. 2003;12:1427–37.
17. Ko HS, von Coelln R, Sriram SR, Kim SW, Chung KK, Pletnikova O, Troncoso J, Johnson B, Saffary R, Goh EL, et al. Accumulation of the authentic parkin substrate aminoacyl-tRNA synthetase cofactor, p38/JTV-1, leads to catechol-aminergic cell death. *J Neurosci*. 2005;25:7968–78.
18. Imam SZ, Zhou Q, Yamamoto A, Valente AJ, Ali SF, Bains M, Roberts JL, Kahle PJ, Clark RA, Li S. Novel regulation of parkin function through c-Abl-mediated tyrosine phosphorylation: implications for Parkinson's disease. *J Neurosci*. 2011;31:157–63.
19. Hainmueller T, Bartos M. Dentate gyrus circuits for encoding, retrieval and discrimination of episodic memories. *Nat Rev Neurosci*. 2020;21:153–68.
20. Adamowicz DH, Roy S, Salmon DP, Galasko DR, Hansen LA, Masliah E, Gage FH. Hippocampal alpha-synuclein in dementia with Lewy bodies contributes to memory impairment and is consistent with spread of pathology. *J Neurosci*. 2017;37:1675–84.
21. An XL, Zou JX, Wu RY, Yang Y, Tai FD, Zeng SY, Jia R, Zhang X, Liu EQ, Broders H. Strain and sex differences in anxiety-like and social behaviors in C57BL/6J and BALB/c mice. *Exp Anim*. 2011;60:111–23.
22. Kim H, Shin JY, Lee YS, Yun SP, Maeng HJ, Lee Y. Brain endothelial p-glycoprotein level is reduced in Parkinson's disease via a vitamin D receptor-dependent pathway. *Int J Mol Sci*. 2020;21.
23. Kim C, Ho DH, Suk JE, You S, Michael S, Kang J, Joong Lee S, Masliah E, Hwang D, Lee HJ, Lee SJ. Neuron-released oligomeric alpha-synuclein is an endogenous agonist of TLR2 for paracrine activation of microglia. *Nat Commun*. 2013;4:1562.
24. Mao X, Ou MT, Karuppagounder SS, Kam TI, Yin X, Xiong Y, Ge P, Umanah GE, Brahmachari S, Shin JH et al. Pathological alpha-synuclein transmission initiated by binding lymphocyte-activation gene 3. *Science*. 2016;353.
25. Shi M, Liu C, Cook TJ, Bullock KM, Zhao Y, Ginghina C, Li Y, Aro P, Dator R, He C, et al. Plasma exosomal alpha-synuclein is likely CNS-derived and increased in Parkinson's disease. *Acta Neuropathol*. 2014;128:639–50.

Publisher's note

Springer Nature remains neutral with regard to jurisdictional claims in published maps and institutional affiliations.